International Conference on Control, Engineering & Information Technology (CEIT ' 14)
Proceedings - Copyright IPCO-2014
ISSN 2356-5608

Variable Speed WECS based on a DFIG and a six-pulse bridge cycloconverter

A.Boumassata, D.Kerdoun,M.Madaci and N.Cherfia
LGEC – Research Laboratory, Department of Electrical Engineering, Constantine 1 University
Constantine, Algeria
e-mail: a_boumassata@yahoo.fr, kerdjallel@yahoo.fr, zoldaioque@gmail.com, msn822009@live.fr

***Abstract*—In this paper, a six-pulse bridge cycloconverter is applied to control a variable speed wind energy conversion system (WECS) with a doubly fed induction generator (DFIG). The dynamic behavior of the WECS, including the models of the wind turbine, the DFIG, the cycloconverter, and the power control of this system, is investigated. The power control of this system is applied to achieve the maximum power and independent control of stator active and reactive powers. Simulation results are presented, to demonstrate the performance of the proposed system.**

Keywords—Cycloconverter, WECS, DFIG, Wind turbine.

I. INTRODUCTION

One way of generating electricity from renewable sources is to use wind energy, mainly because it is considered to be nonpolluting and economically viable. At the same time, there has been a rapid development of related wind turbine technology [1].

Wind turbine generators (WTGs) used in wind energy conversion system can be devised into two types: fixed speed wind turbine (FSWT) and variable speed wind turbine (VSWT). For the first one, the generator is connected directly to the grid without any intermediate of power electronic converters (PECs), and for the last one, the generator is connected through PECs [2], [3]. Moreover, WTGs based on VSWT has distinct advantages than the traditional FSWT, such as more effective power capture, lower mechanical stress and less power fluctuation [4].

The doubly fed induction generator is widely used for VSWT. The principal advantage of the DFIG is that the power electronic converters equipment only carries a fraction of the total power (20–30%) [5].

Cycloconverter is a kind of power electronic converters, it is designed to convert constant voltage, constant frequency AC power to adjustable voltage adjustable frequency AC power without any intermediate DC link. The basic principle of a cycloconverter was proposed and patented by Hazeltine in 1926 [6]. Cycloconverter is suitable for large AC machines because it has advantages: the first one is high efficiency owing to the simple construction of the main circuit, which consists only of switching devices, the other one is high reliability owing to complete absence of permanent short-circuiting [7], and it has also naturally commutative, and no forced commutation circuits are necessary.

In this paper, the proposed system is constituted of the wind turbine, DFIG, cycloconverter, and power control. The stator of the DFIG is connected directly to the grid while the rotor is connected by three phase cycloconverter. The performance of the proposed system will be tested to prove the maximum power control and the independent control of the stator active and reactive powers using stator-flux oriented control technique.

This paper is organized as follows. The modeling of the wind turbine is provided in Section 2. The DFIG is modeled in Section 3. The modeling of the cycloconverter is given in Section 4. The Power Control of the DFIG is developed in Section 5. Finally, the scheme of the proposed WECS is presented in Fig. 1.

II. MODELING OF THE WIND TURBINE

The mechanical power extracted by the turbine from the wind is defined as:

$$P_t = \frac{1}{2} \cdot \rho \cdot A \cdot C_p(\lambda) \cdot V^3 \qquad (1)$$

Where

ρ is the air density, $A=\pi.R^2$ is the rotor swept area, R is the turbine radius, C_p is the power coefficient, λ is the tip speed ratio, and V is the wind speed.

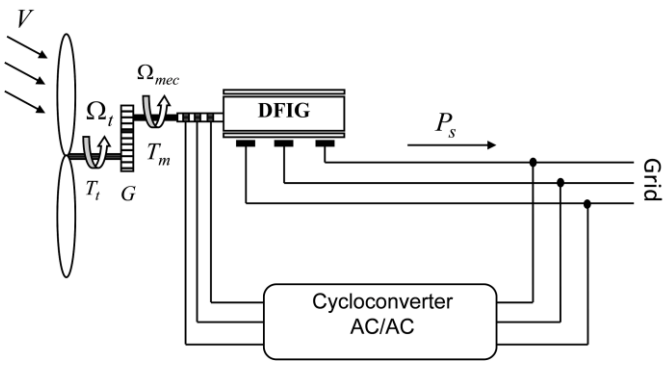

Fig. 1. The proposed system includes cycloconverter.

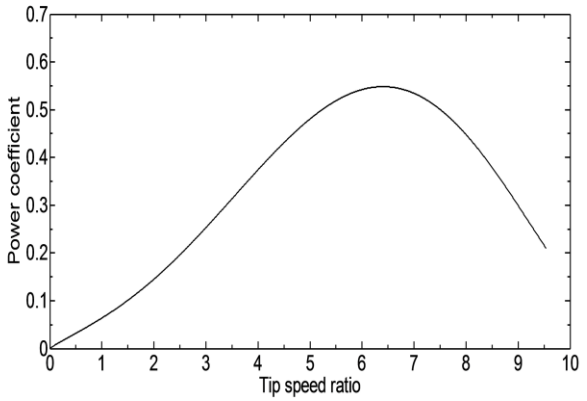

Fig. 2. The power coefficient of the wind turbine.

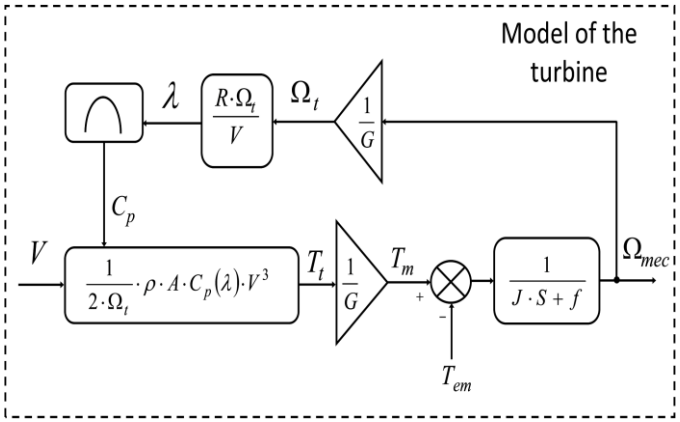

Fig. 3. Model of the turbine.

The power coefficient C_p represents the aerodynamic efficiency of the wind turbine. It depends on the tip speed ratio λ. The tip speed ratio is given as:

$$\lambda = \frac{\Omega_t \cdot R}{V} \tag{2}$$

With Ω_t is the turbine speed.

For our example the power coefficient C_p is given by the following equation [8]:

$$C_p(\lambda) = 7.9563 \cdot 10^{-5} \cdot \lambda^5 - 17.375 \cdot 10^{-4} \cdot \lambda^4 + 9.86 \cdot 10^{-3} \cdot \lambda^3 - 9.4 \cdot 10^{-3} \cdot \lambda^2 + 6.38 \cdot 10^{-2} \cdot \lambda + 0.001 \tag{3}$$

Fig.2, illustrate the curve of C_p *(λ)* obtained by (3).

The maximum value of C_p (C_{p_max} = *0.5483*) is for λ = *6.4*

The turbine torque can be written as:

$$T_t = \frac{P_t}{\Omega_t} \tag{4}$$

The mechanical speed of the generator and the torque of the turbine referred to the generator are given by:

$$\Omega_{mec} = \Omega_t \cdot G \quad \text{and} \quad T_m = \frac{T_t}{G} \tag{5}$$

The mechanical equation of the system can be characterized by:

$$J \cdot \frac{d\Omega_{mec}}{dt} = T_m - T_{em} - f \cdot \Omega_{mec} \tag{6}$$

Where

J is the equivalent total inertia of the generator shaft, *f* is the equivalent total friction coefficient and T_{em} is the electromagnetic torque.

Fig.3, represents the model of the turbine.

The expression of the optimal mechanical power is given by:

$$P_{mec\_opt} = \frac{C_{p\_mex}}{\lambda^3_{Cp\_\max}} \cdot \frac{\rho \cdot \pi \cdot R^5}{2} \cdot \frac{\Omega^3_{mec}}{G^3} \tag{7}$$

III. MODELING OF THE DFIG

The electrical equations of the DFIG in the (d–q) Park reference frame are given by [9]:

$$\begin{cases} V_{sd} = R_s \cdot I_{sd} + \dfrac{d\phi_{sd}}{dt} - \dot{\theta}_s \cdot \phi_{sq} \\ V_{sq} = R_s \cdot I_{sq} + \dfrac{d\phi_{sq}}{dt} + \dot{\theta}_s \cdot \phi_{sd} \\ V_{rd} = R_r \cdot I_{rd} + \dfrac{d\phi_{rd}}{dt} - \dot{\theta}_r \cdot \phi_{rq} \\ V_{rq} = R_r \cdot I_{rq} + \dfrac{d\phi_{rq}}{dt} + \dot{\theta}_r \cdot \phi_{rd} \end{cases} \tag{8}$$

$$\begin{cases} \phi_{sd} = L_s \cdot I_{sd} + M \cdot I_{rd} \\ \phi_{sq} = L_s \cdot I_{sq} + M \cdot I_{rq} \\ \phi_{rd} = L_r \cdot I_{rd} + M \cdot I_{sd} \\ \phi_{rq} = L_r \cdot I_{rq} + M \cdot I_{sq} \end{cases} \tag{9}$$

Where

R_s and R_r are the stator and rotor resistances, respectively. θ_s and θ_r are, respectively, the stator and rotor field angles. L_s, L_r and M are, respectively, the cyclic stator, rotor and mutual inductances.

The active and reactive powers equations at the stator are written as:

$$\begin{cases} P_s = V_{sd} \cdot I_{sd} + V_{sq} \cdot I_{sq} \\ Q_s = V_{sq} \cdot I_{sd} - V_{sd} \cdot I_{sq} \end{cases} \tag{10}$$

And the electromagnetic torque is expressed as:

$$T_{em} = p \cdot (\phi_{sd} \cdot I_{sq} - \phi_{sq} \cdot I_{sd}) \tag{11}$$

With *p* is the number of pole pairs.

IV. MODELING OF THE CYCLOCONVERTER

The cycloconverter is composed of 36 thyristors. Each phase is composed of two back to back rectifiers. The delay angles of those rectifiers are modulated so as to provide an AC output voltage at the desired frequency and amplitude. The rotor is supplied by a three phase cycloconverter.

Fig.4, represents the diagram of three phase-three phase 6-pulse bridge cycloconverter.

This cycloconverter has natural commutation without circulating current. All the thyristors are supposed as idealized.

The switching function in Fig. 4 is defined as:

$$S_{K_{ijk}} = \begin{cases} 1 & S_{K_{ijk}} \ \ is\ closed \\ 0 & S_{K_{ijk}} \ \ is\ open \end{cases} \tag{12}$$

Where

$$K \in \{P, N\},\ i \in \{a, b, c\},\ j \in \{A, B, C\},\ and\ k \in \{1,2\}$$

In order to control the output voltage of the cycloconverter, we need to command the thyristor firing pulses. In this paper, cosine-wave crossing technique is selected to generate firing pulses. So we will have three timing waves and three reference waves and a lot of intersection points. We have 36 control circuits for this cycloconverter one for each thyristor. The output voltage of the three phase-three phase 6-pulse bridge cycloconverter can be represented by a 3x3 matrix [T] such as:

$$\begin{bmatrix} v_A \\ v_B \\ v_C \end{bmatrix} = [T] \cdot \begin{bmatrix} v_a \\ v_b \\ v_c \end{bmatrix} \tag{13}$$

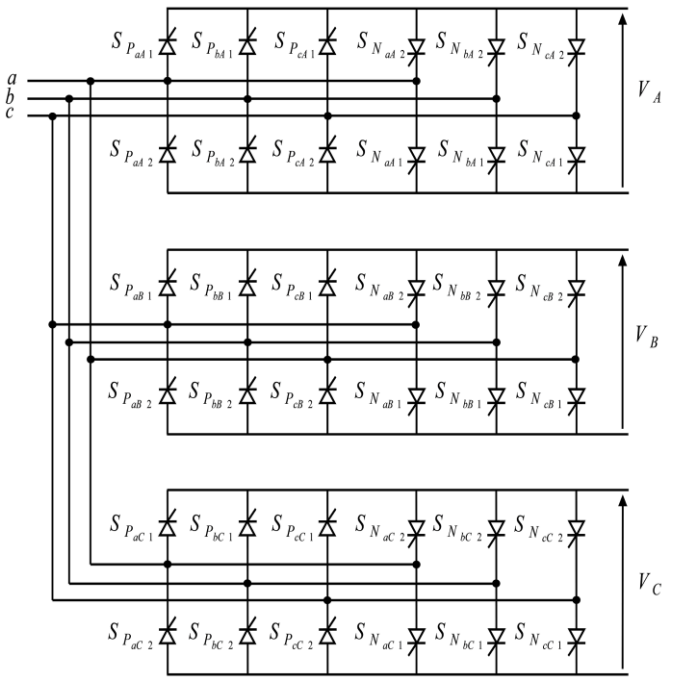

Fig. 4. Three phase-three phase 6-pulse bridge cycloconverter.

$$[T] = \begin{bmatrix} \sum_{\substack{K=P,N \\ k=1,2}} S_{K_{aAk}} & \sum_{\substack{K=P,N \\ k=1,2}} S_{K_{bAk}} & \sum_{\substack{K=P,N \\ k=1,2}} S_{K_{cAk}} \\ \sum_{\substack{K=P,N \\ k=1,2}} S_{K_{aBk}} & \sum_{\substack{K=P,N \\ k=1,2}} S_{K_{bBk}} & \sum_{\substack{K=P,N \\ k=1,2}} S_{K_{cBk}} \\ \sum_{\substack{K=P,N \\ k=1,2}} S_{K_{aCk}} & \sum_{\substack{K=P,N \\ k=1,2}} S_{K_{bCk}} & \sum_{\substack{K=P,N \\ k=1,2}} S_{K_{cCk}} \end{bmatrix} \tag{14}$$

Where

v_a , v_b and v_c are, respectively, the input phase voltages.

v_A, v_B and v_C are, respectively, the output phase voltages.

V. POWER CONTROL

In order to decouple the active and reactive powers, the stator flux victor will be aligned with d-axis ϕ_{sd}, ($\phi_{sd} = \phi_s$ and $\phi_{sq} = 0$). By neglecting resistances of the stator phases the stator voltages will be expressed by [10], [11]:

$$V_{sd} = 0 \quad \text{And} \quad V_{sq} = V_s \approx \omega_s \cdot \phi_s \tag{15}$$

ω_s is the stator pulsation.

The expressions of the statoric currents are written as:

$$\begin{cases} I_{sd} = \dfrac{\phi_{sd} - M \cdot I_{rd}}{L_s} \\ I_{sq} = -\dfrac{M}{L_s} \cdot I_{rq} \end{cases} \tag{16}$$

By replacing these currents in the rotor fluxes equations, we obtain:

$$\begin{cases} \phi_{rd} = \sigma \cdot L_r \cdot I_{rd} + \dfrac{M}{L_s} \cdot \phi_{sd} \\ \phi_{rq} = \sigma \cdot L_r \cdot I_{rq} \end{cases} \tag{17}$$

σ is the leakage coefficient, defined by:

$$\sigma = 1 - \frac{M^2}{L_s \cdot L_r} \tag{18}$$

The rotor voltages can be written according to the rotor currents as:

$$\begin{cases} V_{rd} = R_r \cdot I_{rd} + \sigma \cdot L_r \cdot \dfrac{dI_{rd}}{dt} - s \cdot \omega_s \cdot \sigma \cdot L_r \cdot I_{rq} \\ V_{rq} = R_r \cdot I_{rq} + \sigma \cdot L_r \cdot \dfrac{dI_{rq}}{dt} + s \cdot \omega_s \cdot \sigma \cdot L_r \cdot I_{rd} + s \cdot \dfrac{M \cdot V_s}{L_s} \end{cases} \tag{19}$$

s is the slip of the DFIG.

The electromagnetic torque can be written as:

$$T_{em} = -p \cdot \frac{M}{L_s} \phi_{sd} \cdot I_{rq} \tag{20}$$

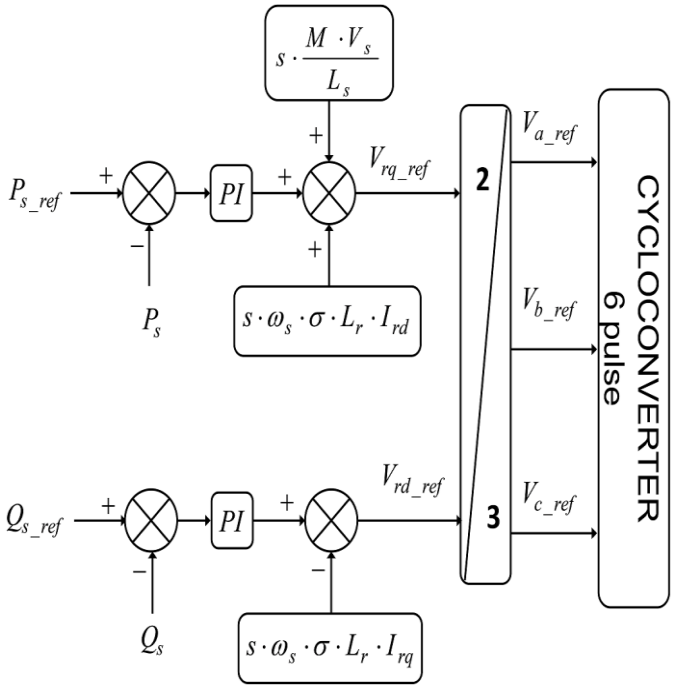

Fig. 5. Stator active and reactive powers control.

And the active and reactive stator powers of the DFIG are expressed by:

$$\begin{cases} P_s = -V_s \cdot \dfrac{M}{L_s} \cdot I_{rq} \\ Q_s = \dfrac{{V_s}^2}{\omega_s \cdot L_s} - V_s \cdot \dfrac{M}{L_s} \cdot I_{rd} \end{cases} \quad (21)$$

Fig.5, represents the simplified diagram blocks of stator active and reactive powers control.

The reference value of the active power exchanged between the stator of the generator and the grid is determined by (7), and it's given by:

$$P_{s\_ref} = -\frac{C_{p\_mex}}{\lambda^3_{Cp\_\max}} \cdot \frac{\rho \cdot \pi \cdot R^5}{2} \cdot \frac{\Omega^3_{mec}}{G^3} \quad (22)$$

The reference value of the stator reactive power, Q_{s_ref} is fixed to zero value to maintain the power factor at unity.

VI. Results and Interpretations

Simulation of the proposed system has been realized using Matlab/Simulink.

The DFIG used in this work is 7.5 KW. It's connected directly through its stator and controlled through its rotor by six-pulse bridge cycloconverter.

Rated parameters: R_s = 0.455 Ω, R_r = 0.62 Ω, L_s = 0.084 *H*, L_r = 0. 081 *H*, *M* = 0.078 *H*, *J* = 0.3125 Kg.m^2, f = 0.00673 N.m.s, p = 2.

Wind turbine parameters are: R (blade radius) = 3 *m*, *G* (Gearbox) = 8, Number of blades = 3.

The variation of the mechanical speed of the DFIG is represented in Fig.6.

Fig. 7, presents the stator active and reactive powers of the DFIG and their references.

Fig. 8, gives the simple waveforms of the stator phase current and voltage, and their zoom.

The rotor phase current and its zoom are showed in Fig. 9. Fig. 10, illustrates the zoom of the rotor phase current and voltage.

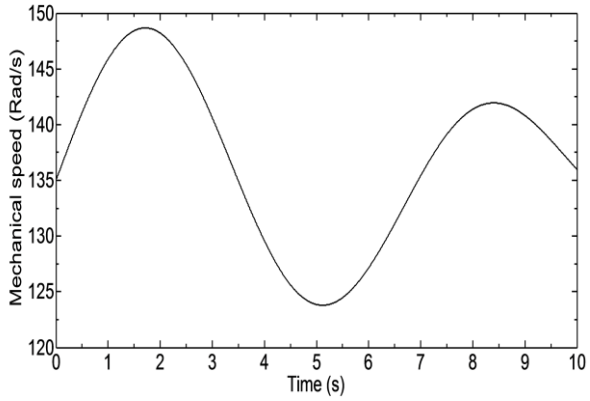

Fig. 6. mechanical speed of the DFIG.

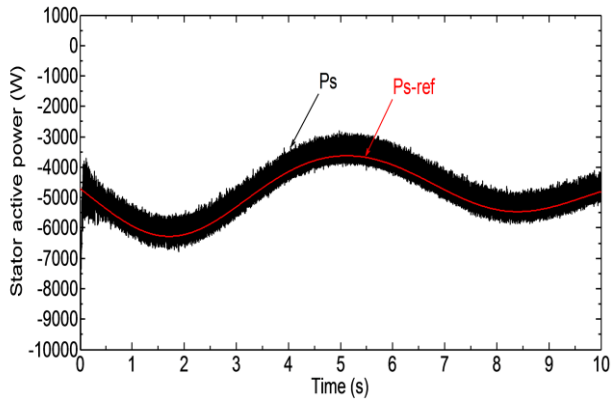

(a)

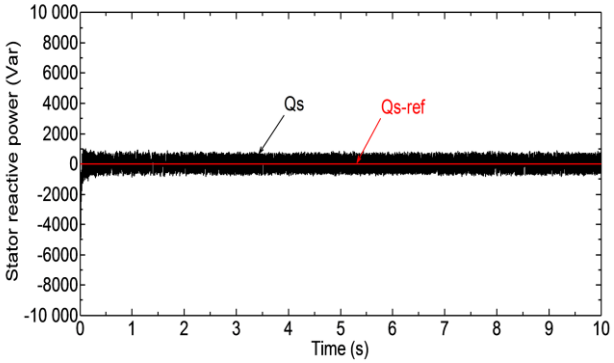

(b)

Fig. 7. (a) Stator active power, (b) Stator reactive power.

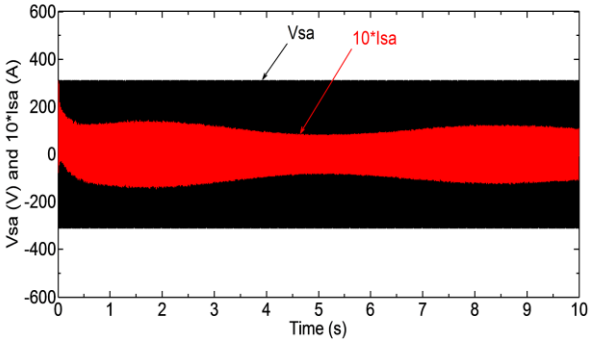

(a)

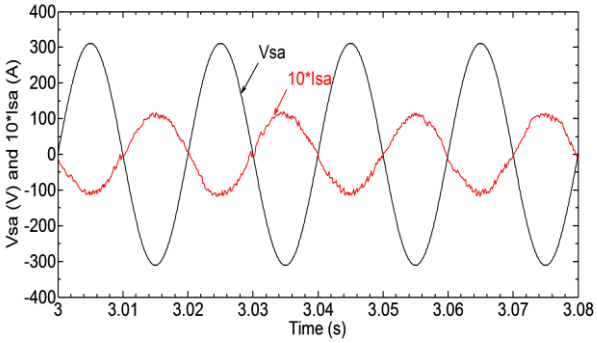

(b)

Fig. 8. (a) Stator phase voltage and current, (b) Zoom of the stator phase voltage and current.

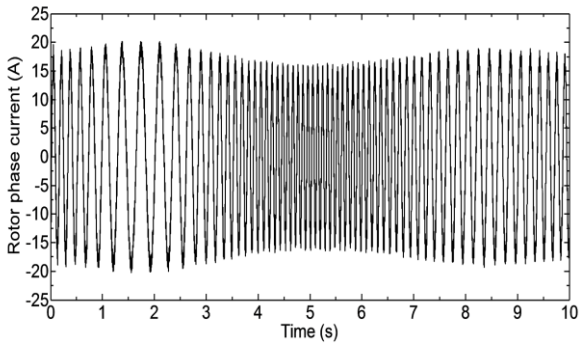

(a)

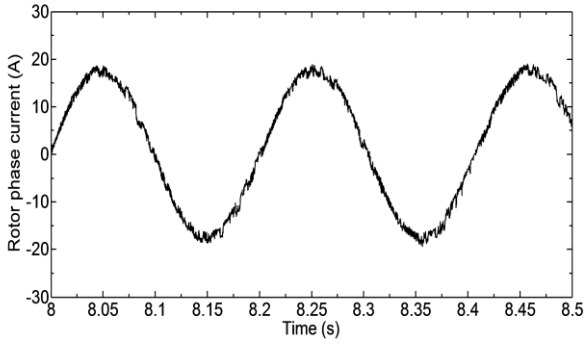

(b)

Fig. 9. (a) Rotor phase current, (b) Zoom of the rotor phase current.

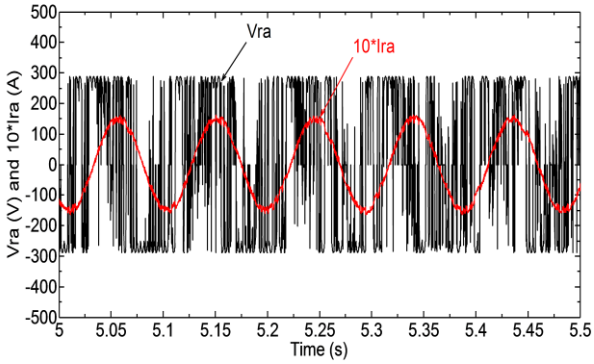

Fig. 10. Zoom of the rotor phase voltage and current.

In Fig.7, the stator active and reactive powers follow their references correctly. This figure validates the power control. The zoom of the stator current and voltage in Fig. 8b, validates the unity power factor. In Fig. 9, the frequency of the rotor phase current is low and varies according to the mechanical speed. The rotor phase current and voltage showed in Fig. 10 validate the control of the cycloconverter.

VII. CONCLUSION

We have presented in this work a variable speed WECS made with DFIG and 6-pulse bridge cycloconverter. The stator of the DFIG is connected directly to the grid while the rotor is supplied by three phase cycloconverter. The maximum power is captured. Simulation results show good decoupling and performance between stator active and reactive powers and guarantee the unity power factor. In this paper, the DFIG with the 6-pulse bridge cycloconverter based on WECS are proved the efficiency and reduced the cost. Finally, the proposed system in this paper is feasible and has many advantages.

REFERENCES

[1] A. Tapia, G.Tapia, J. Xabier Ostolaza and J. Sáenz, "Modeling and control of a wind turbine driven doubly fed induction generator", IEEE Trans. On Energy Conversion, vol. 18, no. 2, June 2003.

[2] M. Tazil, V. Kumar, R.C. Bansal, S. Kong, Z.Y. Dong, W. Freitas and H.D. Mathur, "Three-phase doubly fed induction generators: an overview", IET Electric power applications, vol. 4, 75-89, 2010.

[3] H. S. Kim and D. D.-C. Lu, "Review on wind turbine generators and power electronic converters with the grid-connection issues'', Universities power engineering conference (AUPEC), 20th Australasian, 1-6, 2010.

[4] H. Li, Z. Chen and J. K. Pedersen, "Optimal power control strategy of maximizing wind energy tracking and conversion for VSCF doubly fed induction generator system", Power Electronics and Motion Control Conference, IPEMC, 2006.

[5] K. Ghedamsi and D. Aouzellag, "Improvement of the performances for wind energy conversions systems", Electrical Power and Energy Systems J 2010, 32:936-945.

[6] Y. Liu, G. T. Heydt and R.F. Chu, "The power quality impact of cycloconverter control strategies", IEEE Trans. On Power Delivery, vol. 20, no. 2, April 2005.

[7] S. Miyazawa, F. Nakamura and N. Yamada, "Effective approximation suitable for the control algorithm of microprocessor based cycloconverter", IEE Proceedings, Vol.135, Pt.B, no. 3, May 1988.

[8] Poitier F. ‘‘Etude et commande de generatrices asynchrone pour l’utilisation de l’énergie éolienne’’, Ph.D. thesis, University of Nantes, 19 december 2003.

[9] A. Gaillard, P. Poure, S. Saadate, M. Machmoum, ‘‘Variable speed DFIG wind energy system for power generation and harmonic current mitigation’’, Renew Energy J 2009; 34:1545-1553.

[10] A. M. Kassem, K. M. Hasaneen, A. M. Yousef, “Dynamic modeling and robust power control of DFIG driven by wind turbine at infinite grid”, Int. J. Electrical Power and Energy Systems 2013; 44; 375-382.

[11] L. Jerbi, L. Krichen and A. Ouali, “A fuzzy logic supervisor for active and reactive power control of a variable speed wind energy conversion system associated to a flywheel storage system”, Electric Power Systems Research J 2009, 79:919-925.